

# A cell-based assay to screen stimulators of the Hippo pathway reveals the inhibitory effect of dobutamine on the YAP-dependent gene transcription

Received April 4, 2011; accepted April 22, 2011; published online May 17, 2011

Yijun Bao<sup>1,2</sup>, Kentaro Nakagawa<sup>1</sup>,  
Zeyu Yang<sup>1,3</sup>, Mitsunobu Ikeda<sup>1</sup>,  
Kanchanamala Withanage<sup>1</sup>,  
Mari Ishigami-Yuasa<sup>4</sup>, Yukiko Okuno<sup>4</sup>,  
Shoji Hata<sup>5</sup>, Hiroshi Nishina<sup>5</sup> and  
Yutaka Hata<sup>1,\*</sup>

<sup>1</sup>Department of Medical Biochemistry, Graduate School of Medicine, Tokyo Medical and Dental University, Tokyo 113-8519, Japan; <sup>2</sup>Department of Neurosurgery, First Hospital of China Medical University, Shenyang 110001, China; <sup>3</sup>Department of Ultrasound, Shengjing Hospital of China Medical University, Shenyang 110004, China; <sup>4</sup>Chemical Biology Screening Center, School of Biomedical Science, Tokyo Medical and Dental University, Tokyo 113-8510, Japan; and <sup>5</sup>Department of Developmental and Regenerative Biology, Medical Research Institute, Tokyo Medical and Dental University, Tokyo 113-8510, Japan

\*Yutaka Hata, Department of Medical Biochemistry, Graduate School of Medicine, Tokyo Medical and Dental University, 1-5-45 Yushima, Bunkyo-ku, Tokyo 113-8519, Japan. Tel: +81-3-5803-5164, Fax: +81-3-5803-0121, email: yuhammeh@tmd.ac.jp

The mammalian Hippo pathway is composed of mammalian Ste20-like (MST) kinases and large tumour suppressor (LATS) kinases. Upon the activation of the pathway, MST kinases phosphorylate and activate LATS kinases, which in turn phosphorylate transcriptional co-activators, yes-associated protein (YAP) and transcriptional co-activator with PDZ-binding motif (TAZ), recruit them to the cytosol from the nucleus and turn off cell cycle-promoting and anti-apoptotic gene transcriptions. Thus, the pathway restricts cell overgrowth and prevents tumorigenesis. Although a high cell density and stress signalling are known to activate the pathway, no specific stimulators are so far reported. As the dysfunction of the pathway is frequent in human cancers and correlates with poor prognosis, it is important to find out reagents that stimulate the pathway for not only basic research but also clinical medicine. We here developed a cell-based method of screening reagents that induce the recruitment of YAP to the cytosol. Using this method, we found that dobutamine inhibits the YAP-dependent gene transcription. Contrary to our expectations, the effect of dobutamine is independent of the Hippo pathway but our method opens the possibility to discover Hippo pathway stimulators or Hippo-independent YAP inhibitors.

**Keywords:** gene transcription/green fluorescent protein/signal transduction/tumour suppressor.

**Abbreviations:** DMSO, dimethylsulfoxide; GFP, green fluorescent protein; LATS, large tumour suppressor; MST, mammalian Ste20-like; TAZ, transcriptional co-activator with PDZ-binding motif; YAP, yes-associated protein.

The Hippo pathway regulates cell proliferation and cell death (1–4). It was originally discovered in *Drosophila melanogaster* as a pathway that determines organ size and of which mutations lead to tumorigenesis. The Hippo pathway is activated to stop cell proliferation in normal epithelial cells when cells become confluent. The pathway is also activated by cell stress and induces apoptosis. The mammalian Hippo pathway comprises MST kinases (MST1 and MST2) and LATS kinases (LATS1 and LATS2). When the pathway is activated, MST kinases phosphorylate LATS kinases, which phosphorylate transcriptional co-activators, YAP and TAZ (5–8). YAP and TAZ, when phosphorylated, are recruited from the nucleus to the cytosol, so that the YAP- and TAZ-dependent gene transcriptions are turned off. YAP and TAZ have more than one phosphorylation sites, but Ser127 of YAP and Ser89 of TAZ are the most important determinants of the sub-cellular localization of YAP and TAZ, respectively. As YAP and TAZ mediate the transcription of cell proliferation-promoting and anti-apoptotic genes, the pathway blocks cell proliferation and induces apoptosis. When the Hippo pathway is impaired, YAP and TAZ remain in the nucleus, resulting in tissue overgrowth and tumorigenesis. Disorders of the pathway are very frequently detected in human cancers (9–15). Its down-regulation correlates with the aggressive properties of cancer cells and poor prognosis. Thereby, it is important to find out reagents that stimulate the pathway.

We attempted to establish the method of screening stimulators of the Hippo pathway. In human osteoblastoma U2OS cells, the activation of the Hippo pathway causes the translocation of green fluorescent protein (GFP)-fused YAP from the nucleus to the cytosol. These findings led us to the idea to use U2OS cells expressing GFP-YAP (U2OS-GFP-YAP) to search for stimulators of the Hippo pathway. In order to know how the method works, we tentatively applied a

limited number of well-characterized reagents and examined how the reagents affected the subcellular localization of GFP-YAP. Unexpectedly, we found that dobutamine induces the accumulation of GFP-YAP in the cytosol. This effect of dobutamine turned out to be independent of the Hippo pathway. However, our results suggest that U2OS-GFP-YAP cells are useful to detect reagents that inhibit the YAP-dependent gene transcription.

## Materials and Methods

### DNA constructions

pCneoLATS2-FLAG was described previously (16). pCMV AP is a gift of Sumiko Watanabe (University of Tokyo). 8xGT-IIC- $\delta$ 51LucII (TEAD reporter) and  $\delta$ 51LucII (control) are gifts of Hiroshi Sasaki (Kumamoto University). pCneoFLAG-hWarts was constructed from pCGN hWarts, which is a gift of Hideyuki Saya (Keio University). PCR was performed using H691 (5'-gctagcaagggtgaggaactaaacc-3') and H692 (5'-gcgccgccacgaagtctgtagcc-3') as primers on pUB6/V5-HisA (Invitrogen). The PCR product was digested with NheI/NotI and was ligated into XbaI/NotI sites of pIRES (Clontech) to generate pIRES-blasticidin. PCR was performed using H1674 (5'-atcgatgctcgagctagctctgag-3') and H1675 (5'-actagctcgagaccagctgttcacgacacc-3') as primers on pBudCE (Invitrogen). The PCR product was ligated into ClaI/SpeI sites of pLenti4/TO/DEST (Invitrogen) to generate pLenti-EF vector. pIRES-blasticidin was digested with NotI, filled in and digested with NsiI. pLenti-EF was digested with MluI, filled in and digested with PstI. Ires-blasticidin fragment was ligated to this digested vector. A linker (5'-ctagctcgagaattcacgcgtctcgagatctagatgctgac-3' and 5'-aattgctgactctagatctcgagacgctgaattctgaga-3') was ligated into SpeI/EcoRI sites to generate pLenti-EF-iress-blast vector with multiple cloning sites. NheI/EcoRI fragment from pCneoFH vector was ligated into SpeI/EcoRI sites of pLenti-EF-iress-blast to generate pLenti-EF-FH-iress-blast vector. pLL3.7 vector was digested with XbaI and NotI, filled in and religated to generate pLL3.7 short. NheI/MfeI fragment from pIRES-blasticidin was ligated into NheI/EcoRI sites of pLL3.7 short to generate pLL3.7-iress-blast. pCMV-SPORT6 YAP1 (BC038235, 5747370) was obtained from a commercial source (Open Biosystems). BamHI/EcoRI fragment from pCMV-SPORT6 YAP1 was ligated into BglII/EcoRI sites of pEGFPC3 (Clontech) to generate pEGFPC3 YAP1. NheI/EcoRI fragment from pEGFPC3 YAP1 was ligated into pLL3.7-iress-blast to generate pLL3.7 GFP-YAP1-iress-blast. 1100 bp BamHI/XhoI and 400 bp XhoI/KpnI fragments from pCMV-SPORT6 YAP1 were ligated into BglII/KpnI sites of pCMV-FLAG2 (Kodak) to generate pCMV FLAG-YAP. PCR was performed using H2068 (5'-cgagctcatgctctccagcttctctcag-3') and H1806 (5'-gcgccgctataacatgtaagaagaac-3') as primers on pCMV-SPORT6 YAP1. The PCR product was cloned into pCR4-TOPO vector and 1200 bp SacI/PmeI fragment was isolated. This fragment and 360 bp BamHI/SacI fragment from pCMV-SPORT6 YAP1 were ligated into BglII/SmaI of pCMV-FLAG2 to generate pCMV FLAG-YAP S127A. PCR was performed using H875 (5'-gatagctcgttttagtgaaccgctc-3') and H2352

(5'-gatatacataaccatgtaagaagctt-3') as primers on pCMV FLAG-YAP or pCMV FLAG-YAP S127A. PCR products were digested with NheI/EcoRV and ligated into SpeI/EcoRV sites of pLenti-EF-iress-blast to generate pLenti-EF-FH-YAP-iress-blast and pLenti-EF-FH-YAP S127A-iress-blast.

### Antibodies and reagents

Rabbit anti-phosphorylated LATS1/2 antibody was described previously (16). Rat monoclonal anti-YAP antibody was raised against a synthetic peptide [CTKIDKESFLTWL (single letters code amino acid residues); the N-terminal cysteine is added to conjugate to a key-hole limpet hemocyanin] and purified with protein G-sepharose. Other antibodies were obtained from commercial sources: anti-Myc (9E10) (American Type Culture Collection); mouse monoclonal anti-FLAG M2, mouse monoclonal anti- $\beta$  tubulin and rabbit anti-actin (Sigma-Aldrich); rabbit anti-phospho-YAP and anti-phospho-Thr308-Akt (Cell Signaling); rabbit anti-PARP (BD Pharmingen); mouse monoclonal anti-GFP (Santa Cruz) and peroxidase-conjugated secondary antibodies (MP Biomedicals). Dobutamine hydrochloride, (S)-(-)-propranolol hydrochloride, phentolamine hydrochloride and Hoechst 33342 were obtained from Sigma-Aldrich. Akt inhibitor [1L6-hydroxymethyl-chiro-inositol 2-(R)-2-O-octadecylcarbonate] was purchased from Calbiochem. Forty-eight chemical compounds listed in Table I were purchased from MicroSource Inc.

### Cell cultures and lentivirus production

U2OS cells and HEK293FT cells were cultured in Dulbecco's Modified Eagle Medium containing 10% foetal bovine serum, 100 U/ml of penicillin and 100  $\mu$ g/ml of streptomycin under 5% CO<sub>2</sub> at 37°C. Lentivirus was prepared using HEK293FT cells as described previously (16). U2OS cells were infected with the lentivirus to express GFP-YAP. GFP-positive cells were collected using FACS Vantage (Becton Dickinson). The subcloning was performed by dilution to obtain a single clone.

### RNA interferences

LATS1 and LATS2 were knocked down as described previously (16). The validity of the knockdown was confirmed by RT-PCR (16).

### Reporter assay

HEK293FT cells were plated at  $1 \times 10^5$  cells/24-well plate. Twenty-four hours later, cells were transfected with various combinations of 0.1  $\mu$ g 8xGT-IIC- $\delta$ 51LucII (TEAD reporter), 0.1  $\mu$ g  $\delta$ 51LucII (control), 0.1  $\mu$ g pCMV AP and 0.45  $\mu$ g pLenti-EF-FLAG-YAP-iress-blast. The total amount of DNA was adjusted by adding pLenti-EF-iress-blast. Cells were cultured for 30 h, pre-treated with phentolamine (10  $\mu$ M) or propranolol (10  $\mu$ M) and then treated with dobutamine (10  $\mu$ M). After 18 h incubation, cells were harvested and lysed in the buffer [25 mM Tris/HCl, pH 7.4, 2 mM EDTA, 2 mM DTT, 1% (w/v) Triton X-100, 4 mM MgCl<sub>2</sub>, 4 mM EGTA, 1  $\mu$ g/ml 4-aminodiphenylmethanesulfonyl fluoride hydrochloride and 10% (v/v) glycerol]. Luciferase activity was measured using PicaGene (Toyo INK.). Alkaline phosphatase activity was measured using CDP-Star (Roche) in the assay buffer (98.4 mM glycine, pH 10.5, 1 mM MgCl<sub>2</sub> and 0.1 mM ZnCl<sub>2</sub>).

**Table I. The list of compounds used in this study.**

Aceclidine	Capsaicin	Fampridine	Nicergoline	Siperone
Mesna	Tretinon	Bretyllium tosylat	Foscarnet sodium	Cefsulodin sodium
Carboplatin	Cisplatin	Zisovudine	Azacidine	Cycloheximide <sup>a</sup>
Cyclosporine	Ascorbic acid	Menadione	Salicin	Monensin sodium
Biotin	Aklomide <sup>a</sup>	Nicotinyl alcohol tarta	Floxuridine	Altretamine
Amiprilose	Tiaprind hydrochloride	Bacampillin hydrochloride	Bendro flumethiazide	Bepidil hydrochloride
Trazodone hydrochloride	Menthol(-)	Thonzylamine hydrochloride	Thiamphenicol	Tenoxicam
Dobutamine hydrochloride <sup>a</sup>	Edoxudine	Enoxacin	Meglumine	Pararosaniline pamoate

All compounds were supplied as 10 mM DMSO stock solutions by Chemical Biology Screening Center of Tokyo Medical and Dental University. U2OS-GFP-YAP cells were plated at 100 cells/mm<sup>2</sup>. Forty-eight hours later, the cells were treated with 10  $\mu$ M of the compounds. After 6 h treatment, cells were observed to evaluate the subcellular localization of GFP-YAP. The effect of aklomide is not as remarkable as those of cycloheximide and dobutamine.

<sup>a</sup>Positive compounds.

**Subcellular fractionation**

U2OS-GFP-YAP cells were plated at  $3 \times 10^5$  cells/10 cm dish. Forty-eight hours later, the cells were treated with dobutamine (10  $\mu$ M). After 2 h incubation, the cells were harvested on ice using a cell scraper. The cells were washed with ice-cold PBS twice and resuspended in a 0.5 ml/10 cm dish of TM-2 buffer (10 mM Tris/HCl, pH 7.4 with 2 mM MgCl<sub>2</sub> and 0.5 mM phenylmethanesulfonyl fluoride). The resuspended cells stood at room temperature for 1 min and were incubated on ice for 5 min. Triton X-100 was added to a final concentration of 0.5% (w/v). The cells were incubated on ice for an additional 5 min and sheared by three passages through a 22 gauge needle. The nuclei were examined under a phase-contrast microscope and isolated from the cytosol by centrifugation at 980g for 10 min at 4°C. The pellet was rinsed with 0.5 ml of TM-2 buffer twice and designated as the nuclear fraction. The comparable amount of each fraction was immunoblotted with the indicated antibodies.

**Quantitative analysis of the localization of GFP-YAP in U2OS cells**

U2OS-GFP-YAP cells were plated at  $3.2 \times 10^3$  cells/96-well plate. Forty-eight hours later, cells were pre-treated with phentolamine (10  $\mu$ M) or propranolol (10  $\mu$ M) for 30 min and then treated with dobutamine (10  $\mu$ M). After 6 h incubation, the cells were stained with Hoechst 33342. The images of cells were collected with an imaging cytometry ArrayScan VTI microscope (Cellomics), using algorithms designed with the associated vHCS software. The ratio of nuclear GFP-YAP versus cytoplasmic GFP-YAP was analysed as described previously with some modifications (17). In brief, Hoechst 33342 staining defines the nucleus and enables focusing on the cells within the field. To reduce cytoplasmic contamination within the nuclear area, a nuclear ring 2 pixels inner to the nuclear boundary is drawn to define the nuclear area used for quantitation. The outermost cytoplasmic boundary is drawn 5 pixels beyond the nuclear boundary and the cytoplasmic area used for quantitation is that which lies between nuclear boundary and this outer cytoplasmic annular ring. In both the nuclear and cytoplasmic areas, the intensity of fluorescence of a given protein is averaged throughout the measured area.

**Statistical analysis**

Statistical analyses were performed using the SPSS 13.0 software package (SPSS Inc.). Comparisons between two samples were employed by Student's *t*-test. Multiple comparisons were employed by one-way analysis of variance with Least Significant Difference test as post hoc test, because the homoscedacity assumption was met according to Levene's test.  $P < 0.05$  were considered statistically significant.

**Results****Subcellular localization of green fluorescent protein-fused YAP (GFP-YAP) in U2OS cells**

Upon the activation of the canonical Hippo pathway, MST kinases phosphorylate and activate LATS kinases, which in turn phosphorylate and recruit YAP from the nucleus to the cytosol to shut off the YAP-dependent gene transcription. If GFP-YAP is expressed in cells that harbour the functional Hippo pathway, GFP-YAP should be accumulated in the cytosol under the condition that the pathway is activated. In order to search for Hippo pathway stimulators, we prepared U2OS cells stably expressing GFP-YAP (U2OS-GFP-YAP) and monitored the subcellular localization of GFP-YAP. GFP-YAP localized evenly in the cytosol and in the nucleus in U2OS cells at a low density (Fig. 1A, left). In contrast, GFP-YAP was accumulated in the cytosol in U2OS cells at a high density (Fig. 1A, right). To test whether a compound that stimulates the Hippo pathway indeed induces the cytosolic sequestration in U2OS cells, we used H<sub>2</sub>O<sub>2</sub> as a positive control. H<sub>2</sub>O<sub>2</sub> is known to activate MST kinases (18). We plated U2OS-GFP-YAP cells at a

low density and treated them with H<sub>2</sub>O<sub>2</sub> (1 mM). As expected, GFP-YAP was accumulated in the cytosol after the treatment (Fig. 1B). The knockdown of LATS1 and LATS2 abolished the cytosolic accumulation induced by a high cell density or H<sub>2</sub>O<sub>2</sub> treatment (Fig. 1C). These findings support that the translocation depends on the Hippo signalling. Thus, U2OS-GFP-YAP cells are useful to identify Hippo pathway stimulators.

**Dobutamine induces the recruitment of GFP-YAP from the nucleus to the cytosol**

Before a full-scale screening, we tentatively applied 48 well-characterized chemical compounds to U2OS-GFP-YAP cells (Table I). Three compounds including aklomide, cycloheximide and dobutamine, induced the cytoplasmic translocation of GFP-YAP (Fig. 2A). In order to evaluate the translocation semi-quantitatively, we used a fluorescence imaging-based screening system. As shown in the histogram, dobutamine increased cells with a low nuclear/cytosol GFP signal ratio (Fig. 2B). The effect of dobutamine was the largest (Fig. 2C). Considering the potential molecular link, we here focused on dobutamine. Dobutamine treatment induced GFP-YAP translocation in dose- and time-dependent manners (Fig. 3A). The dobutamine-induced translocation of GFP-YAP was confirmed in the subcellular fractionation (Fig. 3B). The phosphorylation of Ser127 is the most important to determine the cytosolic localization of YAP. The immunoblotting with the antibody, which recognizes the phosphorylated Ser127, demonstrated that GFP-YAP was phosphorylated at Ser127 in response to the dobutamine treatment (Fig. 3C, left). Dobutamine also induced the phosphorylation of endogenous YAP in U2OS cells (Fig. 3C, right). Dobutamine did not induce the translocation of GFP-YAP S127A mutant, in which Ser127 is replaced with alanine (Fig. 3D). This finding supports that dobutamine induces the translocation through the phosphorylation of Ser127.

**Dobutamine suppresses YAP-mediated TEAD reporter activity**

As dobutamine recruits YAP from the nucleus, it is expected to suppress the YAP-dependent gene transcription. YAP interacts with various transcription factors. However, TEAD transcription factors are regarded as the most potent targets of YAP. To test the effect of dobutamine on the YAP-dependent gene transcription, we performed TEAD-responsive luciferase reporter assay. We first transiently expressed GFP-YAP in HEK293FT cells. The effect of dobutamine was not so remarkable as in U2OS cells, but it still induced the translocation of GFP-YAP from the nucleus to the cytosol (data not shown). Therefore, we used HEK293FT cells for the reporter assay. The TEAD reporter exhibited a high activity in the presence of YAP (Fig. 4, Columns 2 and 3). Dobutamine significantly attenuated the YAP-mediated enhancement of the luciferase activity (Fig. 4, Columns 3 and 4).

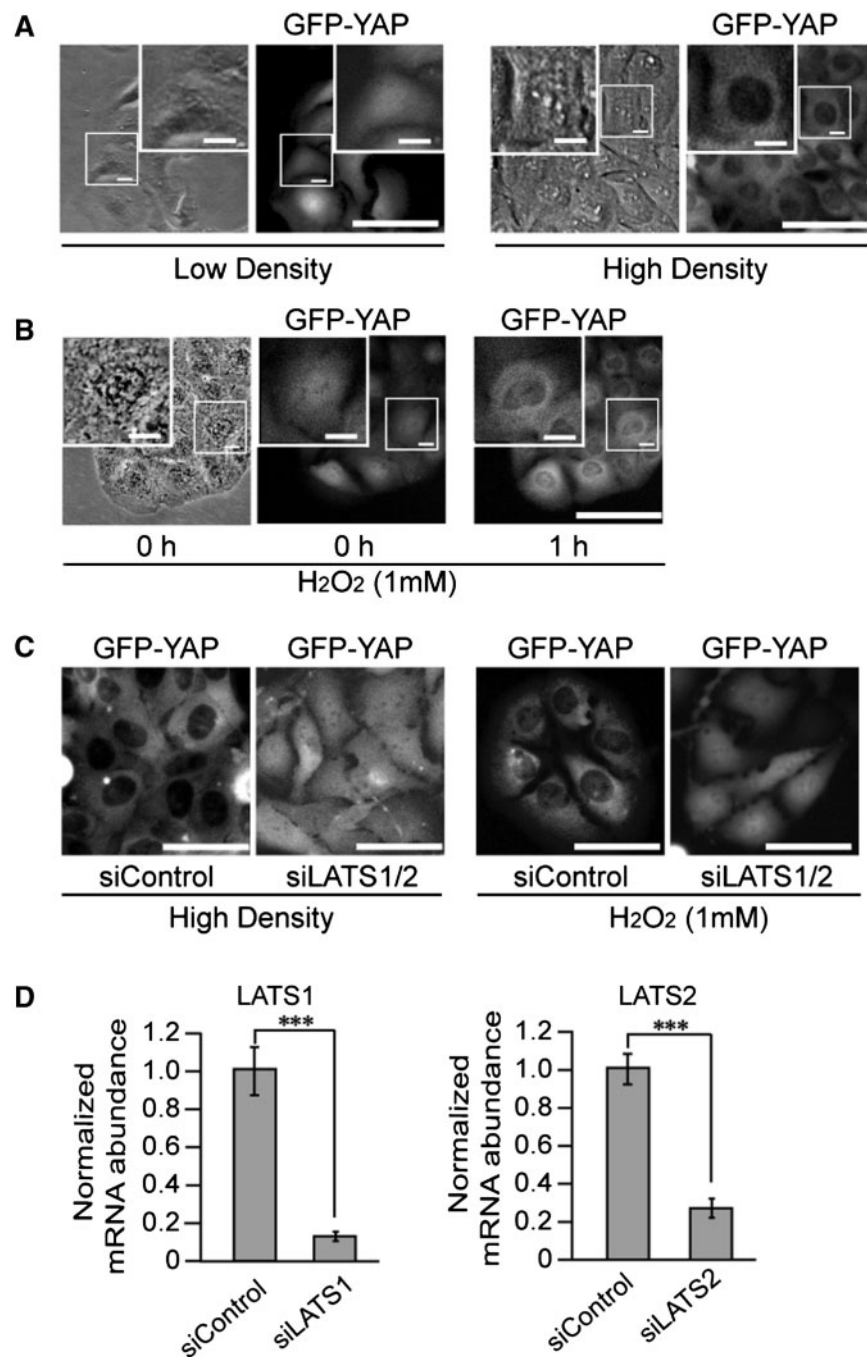


**Fig. 1 YAP localization in U2OS cells.** (A) The effect of the cell density on the subcellular localization of green fluorescent protein (GFP)-fused YAP (GFP-YAP). U2OS cells stably expressing GFP-YAP (U2OS-GFP-YAP) were plated at a low density (100 cells/mm<sup>2</sup>) or at a high density (500 cells/mm<sup>2</sup>). GFP signal was detected evenly in the cytosol and the nucleus at a low density, while it was accumulated in the cytosol at a high density. The left and the right images show the phase contrast image and GFP of the same cells, respectively. Bars, 100  $\mu$ m. Insets show typical cells at higher magnification. Bars in the insets, 15  $\mu$ m. (B) The effect of H<sub>2</sub>O<sub>2</sub> treatment on the subcellular localization of GFP-YAP at a low cell density. U2OS-GFP-YAP cells were plated at 100 cells/mm<sup>2</sup> and treated with H<sub>2</sub>O<sub>2</sub> (1 mM). GFP-YAP was recruited from the nucleus to the cytosol after 1 h treatment. Bars, 100  $\mu$ m. (C) The effect of the knockdown of LATS1 and LATS2 on the subcellular localization of GFP-YAP. When LATS1 and LATS2 were knocked down (siLATS1/2), GFP-YAP remained in the nucleus at a high density (left) and under H<sub>2</sub>O<sub>2</sub> treatment at a low density (right). Bars, 100  $\mu$ m. (D) The validity of LATS1/2 knockdown was confirmed by RT-PCR. Error bars indicate SD of three independent experiments. \*\*\* $P < 0.05$ .

### Dobutamine mediates its effect on YAP through $\beta$ -adrenergic receptor

To confirm that dobutamine works via  $\beta$ -adrenergic receptor, we applied adrenergic receptor inhibitors. A non-specific  $\beta$ -adrenergic receptor inhibitor, propranolol, suppressed the dobutamine-induced phosphorylation

of YAP, whereas a non-specific  $\alpha$ -adrenergic receptor inhibitor, phentolamine, had no effect (Fig. 5A). Likewise, propranolol inhibited the dobutamine-induced translocation of GFP-YAP (Fig. 5B). The quantification using the fluorescence imaging also supported that, propranolol inhibited the dobutamine-induced translocation of

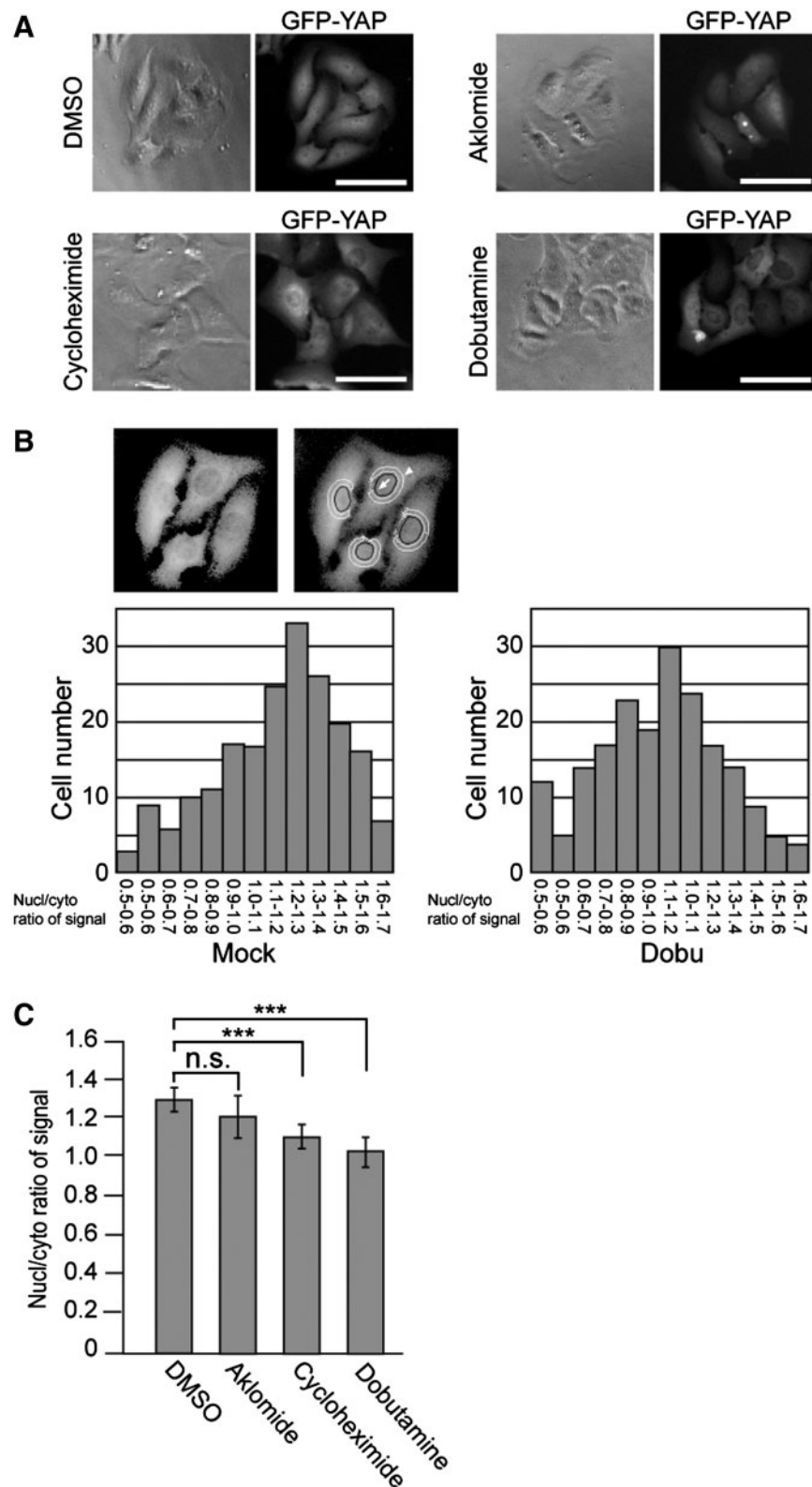


**Fig. 2 Representative images of GFP-YAP in U2OS cells treated with various compounds.** (A) U2OS-GFP-YAP cells were plated at 100 cells/mm<sup>2</sup>. Forty-eight hours later, the cells were treated with various compounds (10  $\mu$ M) listed in Table 1. After 6 h treatment, cells were observed to evaluate the subcellular localization of GFP-YAP. Representative images of the cells treated with dimethylsulfoxide (DMSO), aklomide, cycloheximide or dobutamine. Bars, 100  $\mu$ m. (B) Quantitative analysis of the translocation of GFP-YAP in U2OS cells. The top cell images demonstrate how the nuclear (a black circle, an arrow) and the cytosol (white circles, an arrow head) regions were defined. The analysis was performed using cytometry ArrayScan VTI microscope and algorithms designed with the associated vHCS software. In the histograms, the longitudinal axis shows the cell number, while the horizontal axis shows the ratio of the nuclear/cytosol GFP signal. Dobutamine (Dobu) shifts the histogram to the left, which means that GFP signal in the cytosol increased. More than 100 cells were counted for each well. Four wells were used for each compound and the mean value was calculated for each compound. (C) Quantitative data of the effects of DMSO, aklomide, cycloheximide and dobutamine. Error bars indicate SD of three independent experiments. \*\*\* $P < 0.05$ . n.s., not significant.

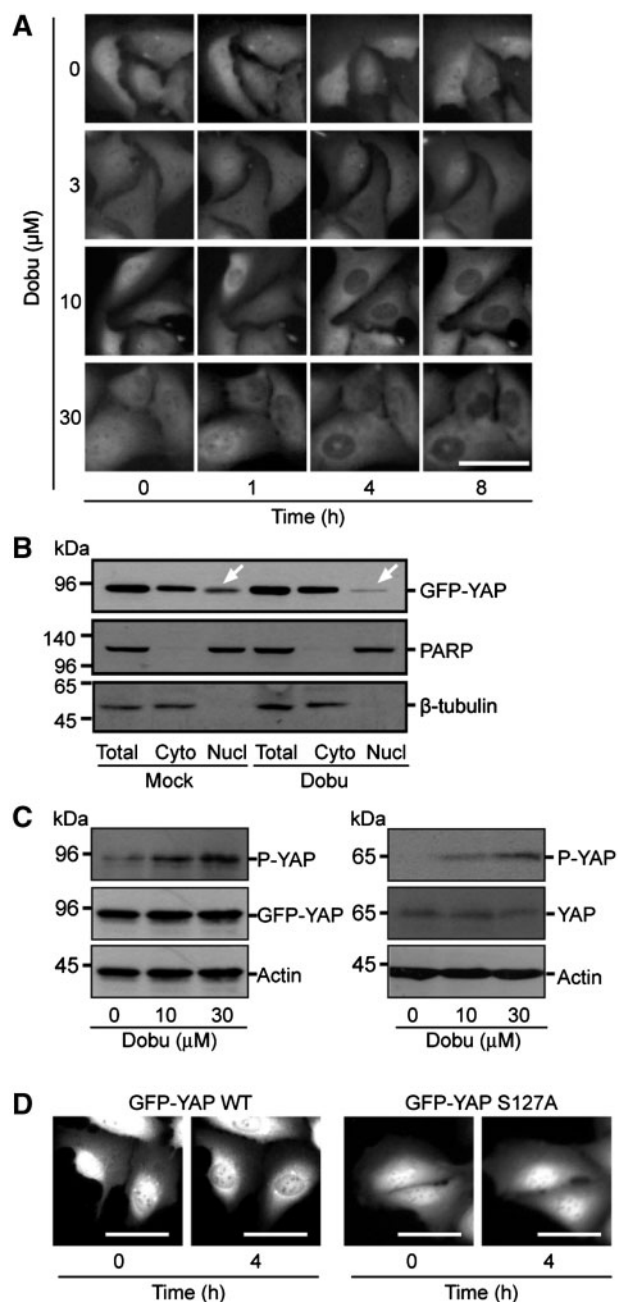


**Fig. 3** The effect of dobutamine on the subcellular localization of GFP-YAP. (A) Time-dependent and dose-dependent effects of dobutamine treatment on the subcellular localization of GFP-YAP in U2OS cells. U2OS-GFP-YAP cells were plated at 100 cells/mm<sup>2</sup>. Forty-eight hours later, the cells were treated with dobutamine (Dobu) (0, 3, 10 or 30 μM) and observed at 0, 1, 4 and 8 h. Dobutamine (3 μM) had no effect (the second panel), while dobutamine (10 and 30 μM) induced the translocation of GFP-YAP (the third and fourth panels). Bar, 100 μm. (B) The subcellular fractionation of U2OS-GFP-YAP cells. U2OS-GFP-YAP cells were plated at  $3 \times 10^5$  cells/10 cm dish. Forty-eight hours later, the cells were treated with either the mock or dobutamine (10 μM). After 2 h incubation, the cells were harvested. The subcellular fractionation was performed to separate the cytosol (Cyto) and the nuclear fraction (Nucl). The comparable amount of each fraction was immunoblotted to detect GFP-YAP, PARP (a nuclear marker) and β-tubulin (a cytosol marker). Dobutamine reduced the nuclear YAP (arrows). (C) The effect of dobutamine on Ser127 phosphorylation of YAP. U2OS-GFP-YAP cells were plated at  $1.5 \times 10^5$  cells/6 cm plate. Forty-eight hours later, the cells were treated with dobutamine (0, 10 or 30 μM). After 1 h treatment, the cells were harvested and immunoblotted with anti-phospho-YAP antibody. Dobutamine

GFP-YAP (Fig. 5C). Consistently, propranolol recovered the dobutamine-induced suppression of the YAP-mediated TEAD reporter activity, while phenolamine had no effect (Fig. 4, Columns 4–6). In conclusion, dobutamine exhibits its action via β-adrenergic receptor.

#### **Neither LATS1/2 nor Akt is involved in the effect of dobutamine**

The kinases that are reported to phosphorylate Ser127 of YAP are LATS kinases and Akt (6–8, 19, 20). Thereby, we hypothesized that dobutamine activates LATS kinases or Akt to phosphorylate YAP. The phosphorylation of LATS1/2 in the activation loop was not enhanced by dobutamine, suggesting that LATS1/2 is not implicated (Fig. 6A, left). Consistently, the knockdown of LATS1 and LATS2 did not influence the dobutamine-induced phosphorylation of YAP (data not shown). The immunoblotting with anti-phosphorylated Akt antibody supported that Akt is activated by dobutamine in U2OS cells (Fig. 6B, right, arrows). We next applied Akt inhibitor to examine whether Akt is necessary for dobutamine to induce the phosphorylation and the translocation of GFP-YAP in U2OS cells. Unexpectedly, Akt inhibitor had no effect on either the phosphorylation or the translocation (Fig. 6B and C, arrows). Akt inhibitor did not abrogate the effect of dobutamine in TEAD reporter assay, either (Fig. 6D). These findings imply that Ser127 of YAP is phosphorylated by an unidentified kinase other than LATS kinases and Akt.

#### **Discussion**

The initial aim of this study is the development of a method for screening stimulators of the mammalian Hippo pathway. The Hippo pathway is activated in a cell density-dependent manner and by stress signals such as oxidative stress and irradiation (1–4). The activation of the mammalian Hippo pathway results in multifaceted molecular events, but the phosphorylation and subsequent translocation of YAP and TAZ is one of the major consequences (5–8). In U2OS cells, GFP-YAP is localized both in the nucleus and in the cytosol at a low cell density, while it is accumulated in the cytosol at a high cell density. The treatment with H<sub>2</sub>O<sub>2</sub> also induces the recruitment of GFP-YAP into the cytosol from the nucleus at a low cell density. Both the recruitments are blocked by the knockdown of LATS1 and LATS2, supporting that GFP-YAP translocates in the Hippo pathway-dependent manner. Thereby, reagents that induce the redistribution of GFP-YAP to the cytosol from the nucleus at a low cell density in U2OS cells are candidates of Hippo pathway stimulators.

induced the phosphorylation of GFP-YAP (left). The same experiment was performed using parent U2OS cells to evaluate the phosphorylation of endogenous YAP (right). (D) The effect of dobutamine on the subcellular localization of YAP S127A. Dobutamine (30 μM) did not induce the translocation of GFP-YAP S127A. Bars, 50 μm.

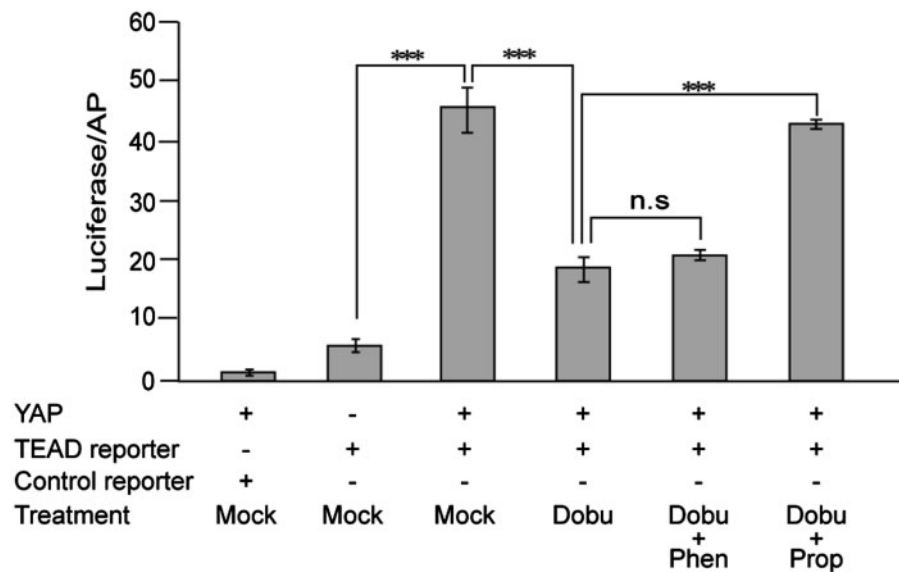


**Fig. 4** The effect of dobutamine on YAP-dependent reporter assay. HEK293FT cells were transfected with various combinations of 8xGT-IIC- $\delta$ 51LucII (TEAD reporter),  $\delta$ 51LucII (control reporter), pCMV AP, and pLenti-EF-FLAG-YAP-ires-blast (YAP). The total amount of DNA was adjusted by adding pLenti-EF-ires-blast. Cells were cultured for 30 h, pre-treated with the mock, phentolamine (10  $\mu$ M) (Phen) or propranolol (10  $\mu$ M) (Prop) and then treated with 10  $\mu$ M dobutamine (Dobu). Luciferase and alkaline phosphatase activities were measured. YAP activated TEAD reporter (Columns 2 and 3). Dobutamine treatment reduced the activity (Columns 3 and 4). Propranolol but not phentolamine blocked the effect of dobutamine (Columns 4–6). Error bars indicate SD of three independent experiments. \*\*\* $P < 0.05$ . n.s., not significant.

In order to understand how the method works, we tested 48 well-characterized reagents. Among them, we found that aklomide, cycloheximide and dobutamine induce the recruitment of GFP-YAP. Aklomide is an anti-coccidial agent used in the veterinary medicine. The effect of aklomide was marginal. Cycloheximide is an inhibitor of protein synthesis, which blocks translational elongation. As cycloheximide blocks the synthesis of many proteins, it could result in various cellular consequences. Indeed, cycloheximide is reported to enhance apoptosis in some cells, but to inhibit it in other cells (21, 22). Dobutamine is a well-known  $\beta$ -adrenergic receptor agonist and is expected to exert a more specific function. Therefore, we here focused on dobutamine. We confirmed the translocation of GFP-YAP in the subcellular fractionation. We also detected the phosphorylation at Ser127 in response to dobutamine treatment for not only GFP-YAP but also endogenous YAP. Moreover, dobutamine attenuated the YAP-dependent TEAD reporter activity in HEK293FT cells. Dobutamine did not induce the translocation of YAP S127A that is a refractory mutant to the Hippo pathway. All these findings support that dobutamine induces the phosphorylation of YAP and the subsequent translocation to the cytosol and inhibits the YAP-dependent gene transcription. We used U2OS cells for the screening, because the translocation of GFP-YAP is clearly detectable in these cells. For instance, GFP-YAP is localized only in the cytosol in mouse breast NMuMG cells even at a low cell density (data not shown). Such cells are not suitable for our screening. However, dobutamine induces the translocation of GFP-YAP and inhibits the YAP-dependent TEAD reporter activity in

HEK293FT cells. Thereby, the effect of dobutamine is not specific for U2OS cells.

Next, we attempted to dissect how dobutamine exerts the inhibitory effect on YAP. Propranolol blocked the effect, while phentolamine did not, indicating that dobutamine mediates its effect via  $\beta$ -adrenergic receptor. Contrary to our expectations, dobutamine did not trigger the phosphorylation of LATS1 and LATS2, which is a hallmark of the Hippo pathway activation. Consistently, the knockdown of LATS1 and LATS2 does not block the dobutamine-induced phosphorylation of GFP-YAP in U2OS cells. Alternatively, dobutamine enhanced the phosphorylation of Akt. Akt is known to phosphorylate Ser127 of YAP in some cells and recruit YAP to the cytosol. YAP mediates the transcription of pro-apoptotic genes in such cells and Akt blocks them to promote cell survival (19, 20). We hypothesized that dobutamine induces the phosphorylation of YAP through Akt in U2OS cells. However, Akt inhibitor did not affect the phosphorylation or translocation of YAP. The findings imply that Akt is activated by dobutamine in U2OS cells but that Akt is not responsible for the dobutamine-induced phosphorylation of YAP. We speculate that an unknown kinase other than LATS kinases and Akt is herein implicated.

The observation that dobutamine inhibits the YAP-dependent gene transcription is intriguing and the underlying molecular mechanism needs to be identified. However, more importantly, we developed a method of screening YAP inhibitors, if not Hippo pathway stimulators. We succeeded to evaluate the effect of reagents on the subcellular localization of GFP-YAP semi-quantitatively and semi-automatically using a fluorescence detection screening system. The effect of

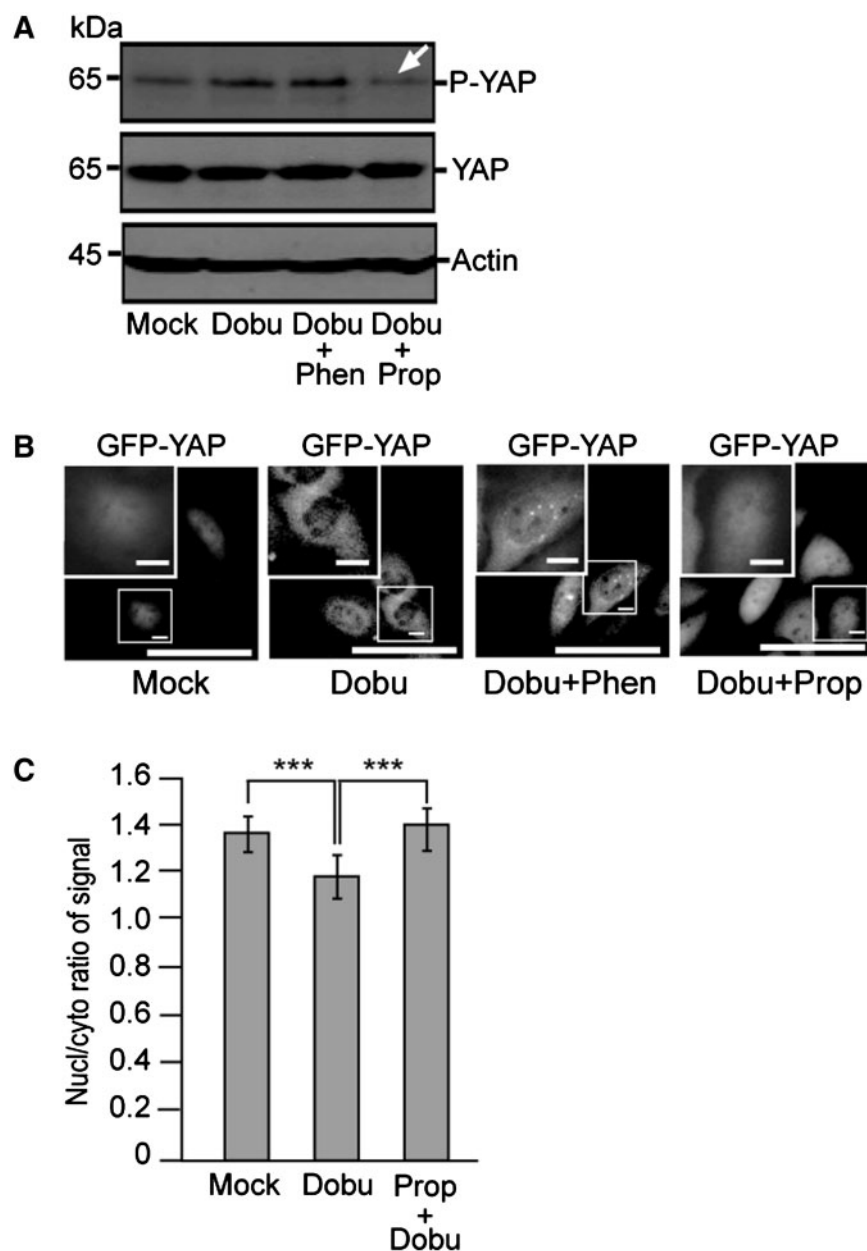


**Fig. 5 The effect of adrenergic receptor inhibitors.** (A) The effect on the dobutamine-induced phosphorylation of YAP. U2OS cells were plated at  $1.5 \times 10^5$  cells/6 cm plate. Forty-eight hours later, the cells were treated with the mock, phentolamine ( $10 \mu\text{M}$ ) (Phen) or propranolol ( $10 \mu\text{M}$ ) (Prop) for 30 min and subsequently treated with the mock or dobutamine ( $10 \mu\text{M}$ ) (Dobu). After 1 h incubation, the cells were immunoblotted with anti-phospho-YAP and anti-YAP antibodies. The immunoblotting with anti-actin was shown to demonstrate that equal amount of the protein was charged onto each lane. Propranolol reduced the dobutamine-induced phosphorylation (an arrow), while phentolamine had no effect. (B) The effect on the translocation of GFP-YAP. U2OS-GFP-YAP cells were plated at  $100 \text{ cells/mm}^2$  in 96-well plate. Forty-eight hours later, the cells were treated with the mock, phentolamine ( $10 \mu\text{M}$ ) (Phen) or propranolol ( $10 \mu\text{M}$ ) (Prop) for 30 min and subsequently treated with the mock or dobutamine ( $10 \mu\text{M}$ ) (Dobu) for 6 h. Propranolol blocked the translocation of GFP-YAP. Bars in the insets and in the large images,  $15 \mu\text{m}$  and  $100 \mu\text{m}$ , respectively. (C) Quantitative data of the effect of propranolol. Error bars indicate SD of three independent experiments. \*\*\* $P < 0.05$ . n.s., not significant.

dobutamine appears to be more impressive when we observe cells in the microscope (Fig. 3A). In the quantitative analysis, the difference between the mock and dobutamine is significant but not so remarkable. We consider that this discrepancy is due to the uneven distribution of cells. Even when cells are plated at a low cell density, the cell density sometimes becomes rather high in some part of a well at 48 h, so that GFP-YAP is localized in the cytosol, which causes the low nuclear/cytoplasmic ratio in the mock-treated samples. The result

that GFP-YAP is detected in the cytosol in the subcellular fractionation is consistent with this assumption (Fig. 3B). When cells are directly observed under a microscope, we can follow the real-time recruitment of GFP-YAP in the same cell. Thereby, the direct sighting gives better resolution. However, in order to test a large number of compounds, the semi-automatic analysis works more efficiently. We have decided to use the fluorescence detection screening system for the first screening and to check cells directly under the



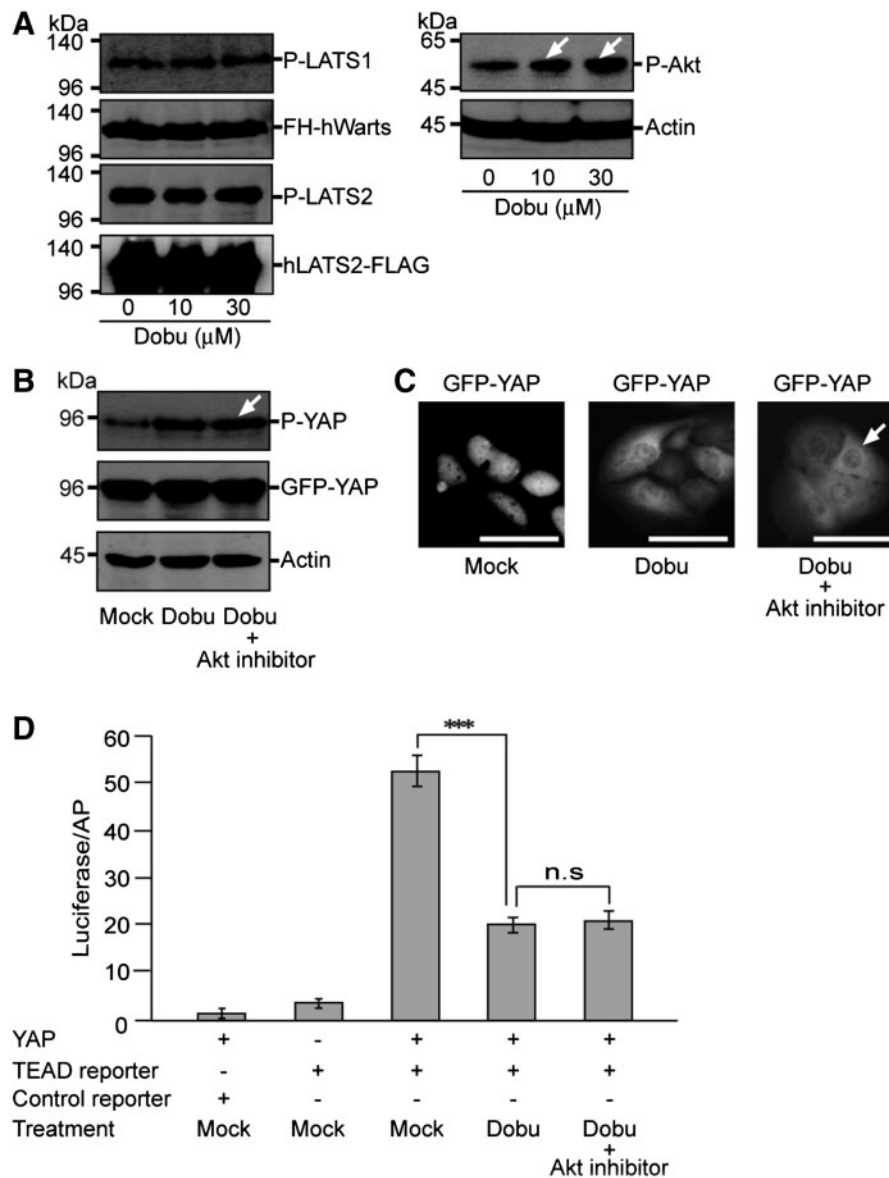


**Fig. 6 Dobutamine activates Akt but Akt is not involved in the translocation of YAP.** (A) The effect of dobutamine on the phosphorylation of LATS1/2 and Akt. U2OS cells were treated with dobutamine (10  $\mu$ M) (Dobu). After 1 h incubation, the cells were immunoblotted with anti-phospho-LATS1/2 and anti-phospho-Akt antibodies. To evaluate the phosphorylation of LATS1 and LATS2, LATS1 or LATS2 was exogenously expressed in U2OS cells. The second and fourth panels show the immunoblotting with anti-FLAG antibody to demonstrate the expression of LATS1 (FH-hWarts) and LATS2 (LATS2-FLAG). Dobutamine increased the phosphorylation of Akt (arrows) but not of LATS1 or LATS2. (B) The effect of Akt inhibitor on the phosphorylation of YAP. U2OS-GFP-YAP cells were pre-treated with the mock or Akt inhibitor (10  $\mu$ M) for 30 min and then incubated with the mock or dobutamine (10  $\mu$ M) (Dobu) for 1 h. The phosphorylation of YAP was not reduced by Akt inhibitor (an arrow). (C) The effect of Akt inhibitor on the translocation of YAP. U2OS-GFP-YAP cells were plated at 100 cells/ $\text{mm}^2$  in 96-well plate. Forty-eight hours later, the cells were treated with the mock or dobutamine (10  $\mu$ M) (Dobu) for 6 h. Akt inhibitor did not block the translocation of GFP-YAP an arrow. Bars, 100  $\mu$ m. (D) The effect of Akt inhibitor on the reporter assay. The reporter assay was performed as described for Fig. 4. Akt inhibitor did not recover TEAD reporter under the treatment of dobutamine (Columns 4 and 5). Error bars indicate SD of three independent experiments. \*\*\* $P < 0.05$ . n.s., not significant.

microscope for the confirmation. We have now launched a large scale screening to identify YAP inhibitors or Hippo pathway stimulators.

## Acknowledgements

We are grateful for Hiroshi Sasaki (Kumamoto University), Sumiko Watanabe (University of Tokyo) and Hideyuki Saya (Keio University) for the materials.

## Funding

Ministry of Education, Sports, Science and Technology (17081008) and Japan Society for the Promotion of Science (JSPS) (22790275, 22590267). Japanese Government (Monbukagakusho) (MEXT) scholarship to Y.B. and Z.Y. TAKASE foundation scholarship to K.W.

## Conflict of interest

None declared.

## References

- Bao, Y., Hata, Y., Ikeda, M., and Withanage, K. (2011) Mammalian Hippo pathway: from development to cancer and beyond. *J. Biochem.* **149**, 361–379
- Pan, D. (2010) The hippo signaling pathway in development and cancer. *Dev. Cell* **19**, 491–505
- Zhao, B., Li, L., and Guan, K.L. (2010) Hippo signaling at a glance. *J. Cell Sci.* **123**, 4001–4006
- Chan, S.W., Lim, C.J., Chen, L., Chong, Y.F., Huang, C., Song, H., and Hong, W. (2011) The Hippo pathway in biological control and cancer development. *J. Cell. Physiol.* **226**, 928–939
- Huang, J., Wu, S., Barrera, J., Matthews, K., and Pan, D. (2005) The Hippo signaling pathway coordinately regulates cell proliferation and apoptosis by inactivating Yorkie, the Drosophila homolog of YAP. *Cell* **122**, 421–434
- Wang, K., Degerny, C., Xu, M., and Yang, X.J. (2009) YAP, TAZ, and Yorkie: a conserved family of signal-responsive transcriptional coregulators in animal development and human disease. *Biochem. Cell Biol.* **87**, 77–91
- Oh, H. and Irvine, K.D. (2010) Yorkie: the final destination of Hippo signaling. *Trends Cell Biol.* **20**, 410–417
- Hong, J.H. and Yaffe, M.B. (2006) TAZ: a  $\beta$ -catenin-like molecule that regulates mesenchymal stem cell differentiation. *Cell Cycle* **5**, 176–179
- Overholtzer, M., Zhang, J., Smolen, G.A., Muir, B., Li, W., Sgroi, D.C., Deng, C.X., Brugge, J.S., and Haber, D.A. (2006) Transforming properties of YAP, a candidate oncogene on the chromosome 11q22 amplicon. *Proc. Natl. Acad. Sci. USA* **103**, 12405–12410
- Jiang, Z., Li, X., Hu, J., Zhou, W., Jiang, Y., Li, G., and Lu, D. (2006) Promoter hypermethylation-mediated down-regulation of LATS1 and LATS2 in human astrocytoma. *Neurosci. Res.* **56**, 450–458
- Takahashi, Y., Miyoshi, Y., Takahata, C., Irahara, N., Taguchi, T., Tamaki, Y., and Noguchi, S. (2005) Down-regulation of LATS1 and LATS2 mRNA expression by promoter hypermethylation and its association with biologically aggressive phenotype in human breast cancers. *Clin. Cancer Res.* **11**, 1380–1385
- Seidel, C., Schagdarsurengin, U., Blümke, K., Würfl, P., Pfeifer, G.P., Hauptmann, S., Taubert, H., and Dammann, R. (2007) Frequent hypermethylation of MST1 and MST2 in soft tissue sarcoma. *Mol. Carcinog.* **46**, 865–871
- Steinhardt, A.A., Gayyed, M.F., Klein, A.P., Dong, J., Maitra, A., Pan, D., Montgomery, E.A., and Anders, R.A. (2008) Expression of Yes-associated protein in common solid tumors. *Hum. Pathol.* **39**, 1582–1589
- Minoo, P., Zlobec, I., Baker, K., Tornillo, L., Terracciano, L., Jass, J.R., and Lugli, A. (2007) Prognostic significance of mammalian sterile20-like kinase 1 in colorectal cancer. *Mod. Pathol.* **20**, 331–338
- Xu, M.Z., Yao, T.J., Lee, N.P., Ng, I.O., Chan, Y.T., Zender, L., Lowe, S.W., Poon, R.T., and Luk, J.M. (2009) Yes-associated protein is an independent prognostic marker in hepatocellular carcinoma. *Cancer* **115**, 4576–4585
- Ikeda, M., Kawata, A., Nishikawa, M., Tateishi, Y., Yamaguchi, M., Nakagawa, K., Hirabayashi, S., Bao, Y., Hidaka, S., Hirata, Y., and Hata, Y. (2009) Hippo pathway-dependent and -independent roles of RASSF6. *Sci. Signal.* **2**, ra59
- Ding, G.J., Fischer, P.A., Boltz, R.C., Schmidt, J.A., Colaianni, J.J., Gough, A., Rubin, R.A., and Miller, D.K. (1998) Characterization and quantitation of NF- $\kappa$ B nuclear translocation induced by interleukin-1 and tumor necrosis factor- $\alpha$ . Development and use of a high capacity fluorescence cytometric system. *J. Biol. Chem.* **273**, 28897–28905
- Takeya, H., Onose, R., and Osada, H. (1998) Caspase-mediated activation of a 36-kDa myelin basic protein kinase during anticancer drug-induced apoptosis. *Cancer Res.* **58**, 4888–4894
- Downward, J. and Basu, S. (2008) YAP and p73: a complex affair. *Mol. Cell* **32**, 749–750
- Basu, S., Totty, N.F., Irwin, M.S., Sudol, M., and Downward, J. (2003) Akt phosphorylates the Yes-associated protein, YAP, to induce interaction with 14-3-3 and attenuation of p73-mediated apoptosis. *Mol. Cell* **11**, 11–23
- Fulda, S., Meyer, E., and Debatin, K.M. (2000) Metabolic inhibitors sensitize for CD95 (APO-1/Fas)-induced apoptosis by down-regulating Fas-associated death domain-like interleukin 1-converting enzyme inhibitory protein expression. *Cancer Res.* **60**, 3947–3956
- Sánchez, A., Alvarez, A.M., Benito, M., and Fabregat, I. (1997) Cycloheximide prevents apoptosis, reactive oxygen species production, and glutathione depletion induced by transforming growth factor  $\beta$  in fetal rat hepatocytes in primary culture. *Hepatology* **26**, 935–943